Journal of Engineering Science and Technology
Vol. 20, No. 6 (2025) 2002 - 2013

PREDICTING TRAJECTORY AND RSSI FOR PROACTIVE HANDOVER THRESHOLD OPTIMIZATION

AHMAD ZAKI AIMAN ABDUL RASHID, AZITA LAILY YUSOF*

Faculty of Electrical Engineering, Kompleks Kejuruteraan Tuanku Abdul Halim Mu'Adzam Shah, Universiti Teknologi MARA, 40450, Shah Alam, Selangor DE, Malaysia
*Corresponding Author: azita968@uitm.edu.my

Abstract

Unmanned aerial vehicles serving as aerial base stations (UAV-BS) have emerged as a promising solution in 5G and beyond due to their flexibility, improved coverage, and rapid deployment capabilities. However, their integration poses challenge in managing seamless handovers, especially with high user mobility and dynamic signal variations. Traditional fixed handover thresholds are inadequate in such conditions. This paper proposes a proactive handover mechanism that combines user trajectory prediction and received signal strength indicator (RSSI) estimation to optimize the handover threshold dynamically. For trajectory prediction, a long short-term memory (LSTM) network was employed, achieving an average displacement error (ADE) of 0.2359 and final displacement error (FDE) of 0.1834, outperforming existing methods. For RSSI prediction, a Random Forest model with 4000 trees achieved superior performance with a mean absolute error (MAE) of 0.00006, root mean square error (RMSE) of 0.0035, and R^2 of 0.9999. The model also demonstrated efficient computation with training and prediction times of 16.93s and 1.40s, respectively. Based on the predicted values, a refined handover threshold (RSRPTh) range of –60.6 dBm to –61.0 dBm was derived, significantly outperforming the standardized 3GPP range (–95 to –100 dBm) and proving more suitable for UAV-BS deployments.

Keywords: Base stations, Handover, Machine learning, Path planning, Wireless communication.

1. Introduction

The integration of Unmanned Aerial Vehicles (UAVs) in wireless communication has gained considerable attention since 3GPP Release 13, with use cases involving UAVs as user equipment (UAV-UE) or as aerial base stations (UAV-BS). UAV-BS systems have demonstrated potential in enhancing signal coverage in underserved areas, including disaster zones, rural environments, and large public events. However, their deployment introduces complex mobility management challenges, especially concerning handover (HO) processes.

Unlike terrestrial base stations, UAV-BS operate in a 3D environment with smaller coverage areas and dynamic positioning, leading to higher handover frequency, increased ping-pong effects, and greater handover failure rates. Efficient trajectory and signal prediction are thus essential for enabling seamless connectivity and optimized handover performance in UAV-assisted networks.

Recent studies have proposed the use of deep learning models such as LSTM [1], hybrid models which integrates the overfitting convolutional neural network (CNN) [2] with LSTM (CNN-LSTM) [2] and gated recurrent unit (GRU) [3] networks for user trajectory prediction, showing strong performance in sequential mobility modelling. LSTM models, in particular, have shown superior accuracy in capturing long-term dependencies [4]. For Received Signal Strength Indicator (RSSI) prediction, machine learning techniques including k-nearest neighbours (k-NN) [5], hybrid models [6], and support vector machine (SVM) [7] have been employed to improve handover decisions. However, limitations such as overfitting, sensitivity to noise [8], and inefficiency in high-dimensional data environments remain.

Traditional handover threshold schemes, often based on fixed signal power levels (e.g., RSRP/RSRQ) [9], struggle in complex or high-mobility UAV networks. Multi-criteria decision-making (MCDM) [10] approaches have been introduced but are sensitive to input uncertainties and not scalable for real-time UAV-BS scenarios [11]. Given these limitations, this research aims to address the following key questions:

- How accurately can user trajectory be predicted in a UAV-BS environment using LSTM models?
- Can machine learning models, such as Random Forest, effectively predict RSSI values based on trajectory-derived distance inputs?
- What is the optimal handover threshold (RSRPTh) derived from predicted trajectories and RSSI that minimizes handover failures and ping-pong effects in 5G aerial networks?

To address these gaps, this paper proposes a novel proactive handover threshold mechanism that integrates LSTM-based user trajectory prediction with Random Forest-based RSSI prediction. Random forest (RF) was chosen due to its ability to handle high-dimensional data and provide explanations for predictions makes them a preferred choice for this application [12]. Another reason for choosing RF is due to the results from a study made by [13] showing Random Forest (RF) models consistently achieved high accuracy in predicting RSSI with 97.25% outperforming decision trees (83.33%) and linear regression (91.67%) when predicting RSSI based on distance. The predicted user path is used to estimate the distance to UAV-BSs, from which the RSSI is calculated and fed into a Random Forest model to determine optimal handover thresholds dynamically. The main contributions of this paper are as follows:

- A hybrid model combining LSTM and Random Forest for proactive handover threshold estimation.
- A simulation framework that mimics user mobility and signal variation in UAV-BS environments.
- Performance evaluation demonstrating improved handover reliability and reduced failure rates.

The rest of this paper is organized as follows: Section 2 presents the methodology. Section 3 discusses the results. Section 4 concludes the paper.

2. Methodology

The methodology for this research is divided into three parts, namely the trajectory prediction using LSTM, RSSI prediction using Random Forest, and the handover threshold calculation. The flow of the research is illustrated in Fig. 1, where it starts with the trajectory prediction, RSSI prediction, and the handover threshold alongside each of their inputs and outputs, respectively. Both simulations of predicting values (trajectory, RSSI) were made using software such as Visual Studio Code and the Python programming language alongside its libraries such as Pandas, Scikit-Learn, Matplotlib, TensorFlow, NumPy, and Keras. The following section describes the methodology of each phase accordingly.

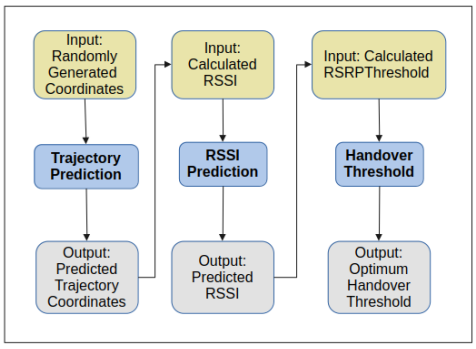

Fig. 1. Illustration of LSTM model layers.

2.1. Trajectory prediction using LSTM

Predicting users trajectories using LSTM starts by generating a random dataset for a single user using the Python programming language with x-coordinates and y-coordinates with starting point at (-500,0) and ends at (550,100) respectively, for 1000 iterations. After generating the dataset for the user trajectory in a CSV file, it is then fed to the LSTM model for predicting the trajectory. LSTM models were developed using Keras's Sequential class through integrating multiple layers, which then transforms it into a deep learning (DL) model. Figure 2 illustrates the LSTM model that was created with five different layers starting with the first LSTM layer with Tanh activation, the primary dropout layer with a minimum value of 0.1, a maximum value of 0.5, and a step value of 0.1, the secondary LSTM layer, the secondary dropout layer with similar parameters as the first one, and lastly, the dense layer with linear activation. The compilation of the model is made using the

optimizer called Adam and varying values of learning rate (e.g., 1.0×10^{-3}, 5.0×10^{-4}, 1.0×10^{-4}).

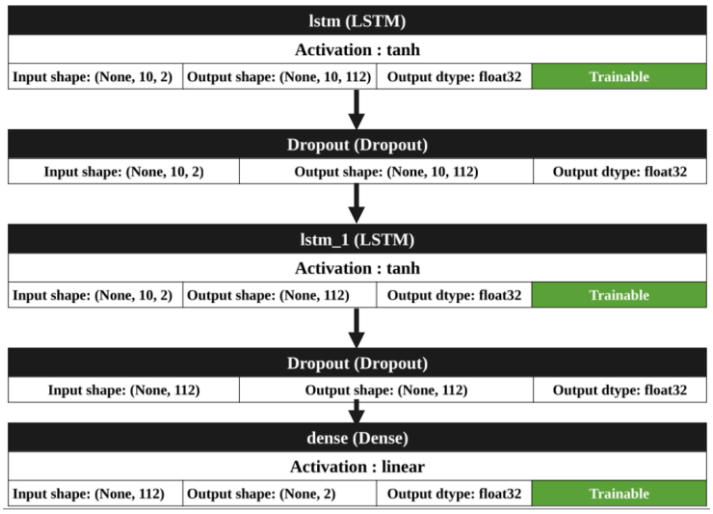

Fig. 2. Illustration of LSTM model layers.

2.2. RSSI prediction using random forest algorithm

In this section, the RSSI prediction utilizing the Random Forest algorithm was discussed, such as the equation for calculating RSSI values and the prediction equation using the Random Forest algorithm. The process starts with calculating the distances between two points (do) as shown in Eq. (1), which consists of past coordinates (x1, y1) and future coordinates (x2, y2) received from the LSTM's trajectory prediction. The distance (do) will then be inserted in the Log-Distance Path Loss Radio model [14] as shown in Eq. (2), where the RSSI at reference distance (d) (RSSI (d)) was configured at -40 dBm, the path loss exponent (n) of 2 indicating free-space propagation, and the reference distance (d) of 1 meter.

$$\boldsymbol{d_o = \sqrt{(x_2 - x_1)^2 + (y_2 - y_1)^2}} \tag{1}$$

$$RSSI(d_O) = RSSI(d) - 10 * n * log\left(\frac{d}{d_o}\right) \tag{2}$$

Once the RSSI values have been calculated for each distance, they will be inserted into the Random Forest algorithm [15] as shown in Eq. (3), where the indicates the predicted value of RSSI, the number of trees (N), and Ti(x) as the prediction made by the ith tree for input (x). The random forest algorithm works by having many decision trees, and each decision tree is trained on a random subset of the data. Each of the three makes a prediction for RSSI based on the input features being provided. Due to the RSSI values being continuous and able to be seen as a regression problem, it averages all three outputs. The simulation for predicting RSSI values was made using the Python programming language, splitting the datasets into training and testing datasets based on the Pareto principle of an 80:20 ratio.

$$\hat{RSSI} = \frac{1}{N}\sum_{i=1}^{N} T_i\,(x) \tag{3}$$

2.3. Handover threshold (RSRP threshold)

The equation for calculating the handover threshold (RSRPTh) is shown in Eq. (4), which consists of the RSSI values calculated previously that subtract the logarithmic part on the right-hand side comprising the physical resource blocks (N). The value of physical resource block (N) was taken from research made in [16], which utilizes UAV-BS bandwidth of 4 MHz, a reduction factor of 0.9, bandwidth of each resource block of 180 kHz, and effective bandwidth of 3.6 MHz, producing a total number of physical resource blocks (N) of 20.

$$RSRP_{th} = RSSI(d_o) - 10log_{10} \quad (4)$$

3. Results and Discussion

The results and discussion for this research follow the methodology categorization, where it starts with the trajectory prediction utilizing LSTM, prediction of RSSI values using Random Forest, and calculated values of handover threshold.

3.1. Trajectory prediction using LSTM

This section illustrates the results and discussions on the users predicted trajectory utilizing the long short-term memory (LSTM) model. Figure 3(a) shows the results from the trajectory prediction utilizing the LSTM model in x,y coordinates, where the actual trajectory is coloured in blue and the predicted trajectory is coloured in red. It can be seen that both the actual and predicted trajectory is directionally aligned where both trajectories follow a similar path, indicating that the model captures the overall motion trend correctly. The small deviation in x and y suggests high prediction accuracy. It can also be seen that the predicted trajectory appears to consistently follow the shape of the actual trajectory, but it slightly underestimates the x-axis components. The y-coordinates are also reasonably close, suggesting the model captures vertical movement accurately. This demonstrates the feasibility of using LSTM-based models for proactive mobility prediction in UAV-BS environments. The consistency in trend alignment shows that the model effectively generalizes motion patterns over time.

Figure 3(b) shows the depiction of the predicted path for two UAV-BSs with overlapping signal coverage. Two circles represent UAV-BS coverage areas centred at (0,0) and (1000,0), with 1000-meter radius. The red cluster shows the LSTM-predicted user trajectory points. The overlapping zone is where the two UAV-BS coverage areas intersect, indicating the handover region. The LSTM has predicted a trajectory that lies in the overlapping region of both UAV-BS. This reason for this illustration is to indicate that the predicted trajectory followed the path for searching the target UAV-BS which are on the right-hand side of the serving UAV-BS cell and does not exceed from the UAV-BS radius. The predicted trajectory lies in the critical handover zone which tells that if a user moving through this area would likely trigger a handover event. This placement supports proactive handover threshold estimation because the model can predict when the users enter this region. Coupled with RSSI estimates, a smart handover decision can be made before signal degradation occurs. This visualization validates the model's spatial accuracy and its utility for real-time mobility-aware handover management in UAV-assisted networks.

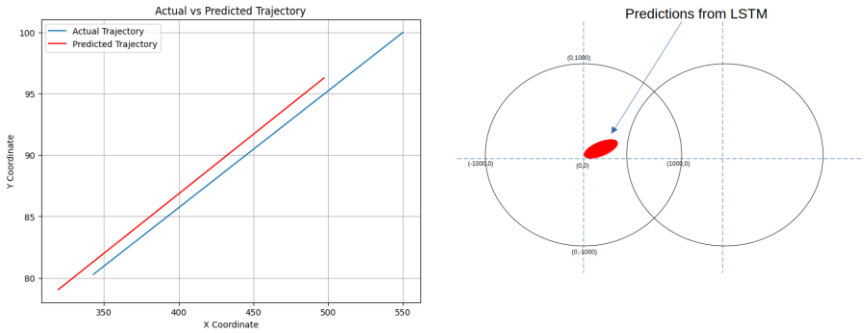

(a) Actual vs Predicted Path with LSTM Model

(b) Depiction of Predicted Trajectory in Two UAV-BS Overlapping Coverage

Fig. 3. Trajectory prediction using LSTM model.

Figure 4 illustrates the RSSI values across predicted trajectories where the x-axis indicates the predicted x-coordinate and y-axis indicates the predicted y-coordinate. The Viridis colormap shows the RSSI values at each predicted coordinate point where the stronger signal with higher RSSI is coloured in yellow, and the weaker signal with weaker RSSI coloured in dark blue and purple. The figure shows strong gradient trend where the RSSI decreases and gets more negative as we move diagonally from bottom-left to top-right. This indicates a clear spatial correlation as the user moves further in a certain direction (e.g. northeast), the RSSI drops, suggesting increasing distance from the UAV-BS impacting signal propagation. The spatial smoothness and lack of outliers suggest that the Random Forest model effectively captures the spatial signal distribution, making it a reliable predictor for handover threshold calculations. From this observation, it can be concluded that the RSSI predictions are spatially coherent and aligned with physical propagation expectations, and these predicted RSSI values are valid inputs for proactive handover threshold.

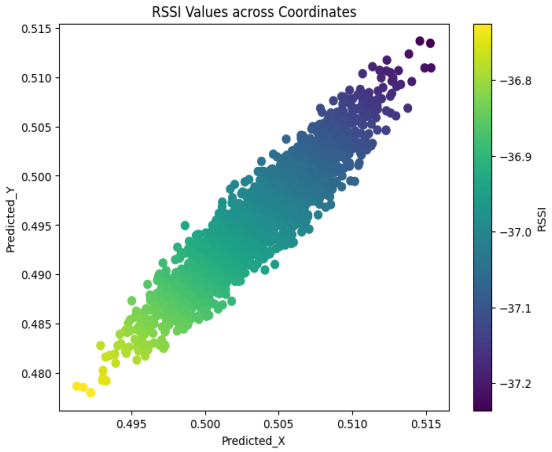

Fig. 4. RSSI values across predicted trajectories.

Table 1 shows the evaluation performance comparison between our LSTM model utilized for trajectory prediction and the LSTM model utilized in [17]. The model was evaluated based on the evaluation metrics such as mean absolute error (MAE), mean squared error (MSE), root mean squared error (RMSE), mean absolute percentage error (MAPE), r-squared (R2), average displacement error (ADE), and final displacement error (FDE). For comparison with the LSTM model in [17], a different dataset was used for standardization purposes. The UCY-ZARA02 dataset [18] was used for predicting the trajectories and produces the results as Table 1. From the comparison, it can be seen that our LSTM model has lower ADE and FDE when compared to the LSTM model in [17], indicating less error when predicting the trajectories and indicating higher prediction accuracy. The reason for this is due to our LSTM model being configured differently from the LSTM model in [17], such as having two LSTM layers, two dropout layers, Tanh activation, ten sequence lengths, a test size of 0.2, an SGD optimizer, 50 epochs, a batch size of 32, and a learning rate of 0.005.

Table 1. Evaluation performance comparison for trajectory prediction.

	Our LSTM Model	LSTM Model [17]
Mean Absolute Error (MAE)	0.254	N/A
Mean Squared Error (MSE)	0.084	N/A
Root Mean Squared Error (RMSE)	0.289	N/A
Mean Absolute Percentage Error (MAPE)	83.6%	N/A
R-Squared (R^2)	37.9%	N/A
Average Displacement Error (ADE)	0.2359	0.4827
Final Displacement Error (FDE)	0.1834	0.7099

3.2. RSSI prediction using random forest

This section shows the discussion of the results produced from the RSSI prediction using the Random Forest algorithm. Figure 5 shows the line chart of actual versus predicted RSSI values using Random Forest (RF) algorithm. The x-axis shows the sample index (e.g. 1 to 40), the y-axis shows the RSSI values in dBm, the blue line shows the actual RSSI values, and the orange line indicates the predicted RSSI values from the RF model. It can be seen that the actual and predicted RSSI lines almost perfectly overlap across all 40 samples. The 40 samples of the sample index represent a subset of the dataset, which indicates the first 40 predictions generated by the RF model configured in the Python programming. This indicates an extremely close match between predicted and actual RSSI values meaning very low prediction error, and strong generalization of the model over individual samples. The fluctuations in RSSI are captured well by the model which shows the spikes and dips in the actual line are mirrored by the predicted line. This shows that the model responses well to dynamic changes in RSSI across different samples. It can be concluded that the model successfully learns non-linear signal behaviours in the environment, and, has minimal underfitting and overfitting over the shown sample range.

Table 2 displays the evaluation performance comparison for RSSI prediction between our random forest model and the random forest model in [18]. For standardization purposes, the dataset used for RSSI prediction for comparison uses the dataset from [19], which is similar to the dataset utilized in [18]. It can be seen

that our random forest model has lower error in terms of MAE and RMSE, better accuracy in terms of higher R-squared value, and lower training and prediction time when compared to the model in [18]. One of the main reasons for this achievement is due to our model utilizing a higher number of trees (e.g., 4000) for prediction, which increases the prediction accuracy and lowers the time for predicting and training.

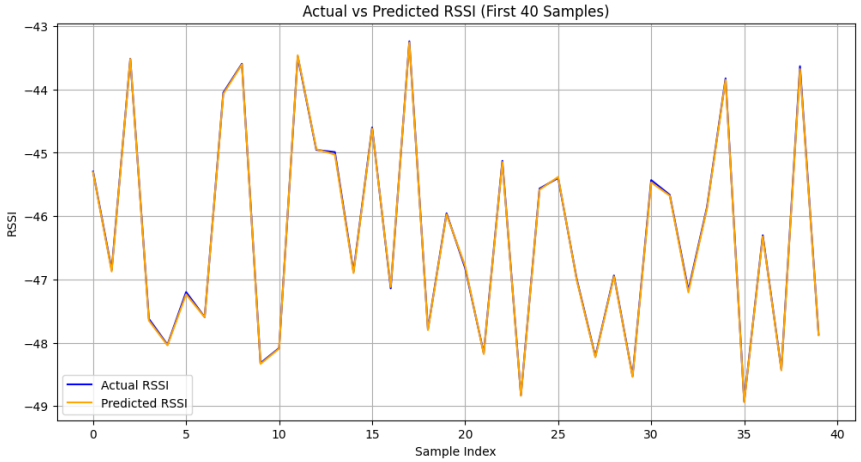

Fig. 5. Actual vs predicted RSSI values using random forest algorithm.

Table 2. Evaluation performance comparison for RSSI prediction.

	Our RF Algorithm (4000 Trees)	**RF Model [18] (3000 Trees)**
Mean Absolute Error (MAE)	0.0006	0.0221
Root Mean Squared Error (RMSE)	0.0035	0.0323
R-Squared (R2)	0.9999	0.9808
Training Time (in seconds)	16.9282	114.7459
Prediction Time (in seconds)	1.4026	5.8427

3.3. Handover threshold calculation

Figure 6 shows the handover threshold ($RSRP_{Th}$) values for 400 datasets which was computed based on the predicted user trajectories and RSSI values. The graph elements consist of the x-axis showing the dataset index (0 – 400), y-axis that shows the handover threshold value ($RSRP_{Th}$) in (dBm), and the line plot showing the variation of calculated handover thresholds across datasets. It can be seen that the range of threshold values that varies between -60.6 dBm to -61.0 dBm approximately showing a relatively narrow, stable threshold range, indicating ideal for minimizing unnecessary handovers.

The plot shows dynamic variation across different datasets which implies the system adapts threshold contextually due to the distance and signal quality. The plotted graph also shows no major outliers or instability. Even with the sharp transitions, the values stay within a small margin, indicating reliable and bounded prediction behaviour. It can be seen that the model is effectively personalizing the

handover threshold for each dataset. The bounded fluctuations suggest the hybrid LSTM and RF is not overly reactive which supports proactive and adaptive handover decisions, thus preventing early or failed handovers. The RSRP threshold achieved in this research was compared with the RSRP threshold standardized by 3GPP in both technical specifications of TS 38.331 and TS 38.304 for 5G networks, which ranges from -95 to -110 dBm. Due to the simulation being based on 5G UAV-BS networks, which consist of high mobility in both UAVs [20, 21] and UEs [24, 25], signal drops frequently occurring suddenly in the air, and the requirement to hand over early when the signal is strong, our handover threshold is more suitable for UAV-BS networks [26, 27].

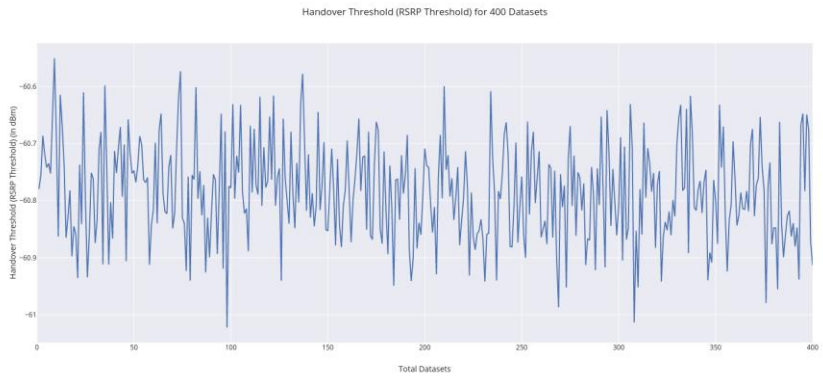

Fig. 6. Handover threshold ($RSRP_{Th}$) for 400 datasets.

Table 3 shows the summarized inference for the results obtained for Figs. 3(a), 3(b), 4, 5 and 6.

Table 3. Tabulation of inference for the results for Figs. 3 (a) and (b), Fig. 4, Fig. 5 and Fig. 6.

Figure	Inference Summary
Figure 3(a)	Figure 3(a) illustrates the predicted trajectory compared to the actual user trajectory. The predicted path closely follows the actual trajectory with minor deviation, particularly along the X-axis, indicating the LSTM model's ability to accurately capture mobility trends. This demonstrates the feasibility of using LSTM-based models for proactive mobility prediction in UAV-BS environments [21]. The consistency in trend alignment shows that the model effectively generalizes motion patterns over time.
Figure 3(b)	Figure 3(b) shows the predicted user trajectory (red ellipse) obtained from the LSTM model, placed within the overlapping coverage region of two UAV-BS located at (0,0) and (1000,0). The trajectory lies within the handover zone, indicating a high likelihood of cell transition. The LSTM model successfully forecasts user movement within this critical area, enabling proactive RSSI prediction and optimized handover threshold computation. This visualization validates the model's spatial accuracy and its utility for real-time mobility-aware handover management in UAV-assisted networks.
Figure 4	Figure 4 illustrates the predicted RSSI values across the predicted user coordinates. The colour gradient reveals a consistent decline in signal strength as the user moves away from the source, reflecting the expected behaviour of wireless signal propagation. The spatial smoothness and lack of outliers suggest that the Random Forest model effectively

captures the spatial signal distribution, making it a reliable predictor for handover threshold calculations.

Figure 5 Figure 5 presents the comparison between actual and predicted RSSI values across the first 40 test samples. The predicted values (orange) closely track the actual measurements (blue), reflecting the model's ability to accurately learn and generalize signal patterns. The high fidelity in matching rapid signal fluctuations further reinforces the model's effectiveness for RSSI prediction in dynamic UAV-BS environments [22], contributing directly to more reliable handover decision-making [23].

Figure 6 Figure 6 illustrates the handover threshold (RSRP) values computed across 400 datasets. The results reveal a tightly bounded fluctuation between –60.6 dBm and –61.0 dBm, reflecting the model's ability to dynamically adjust thresholds based on predicted mobility and signal strength conditions. Despite variability across different input scenarios, the model maintains stable and adaptive thresholds, which is crucial for minimizing ping-pong handovers and reducing failure rates in UAV-BS environments.

4. Conclusions

It can be concluded that the research is capable of obtaining the optimum handover threshold for the utilization of 5G aerial base station networks. The methodologies used for conducting the research start with predicting users trajectories using the LSTM model. Then the predicted trajectories were used to calculate the distance between two points, which is used as the input for calculating RSSI values. The resulting RSSI values were inserted into the random forest algorithm to predict the best RSSI values, which are then used to calculate the handover threshold ($RSRP_{Th}$). The trajectory prediction using LSTM was compared with other researchers and produced better average displacement error and final displacement error. The RSSI prediction using Random Forest was compared with other research and produced lower errors, higher prediction accuracy, and better training and prediction time. The calculation of handover threshold when compared to the standard 3GPP handover threshold indicates great suitability for 5G aerial base station networks. Future works would use the following handover threshold in a handover algorithm with 5G aerial base station networks.

Acknowledgement

This paper is part of research work supported by the Ministry of Higher Education (MOHE) for the funding under the FRGS Grant File no.: FRGS/1/2024/TK07/UITM/02/6 and Faculty of Electrical Engineering, Universiti Teknologi MARA, Shah Alam.

Nomenclatures

d_o	Distances between two points
d	Reference distance
n	Path Loss Exponent
$RSRP_{th}$	Handover Threshold (RSRP Threshold)

Greek Symbols

^	Predicted Value (e.g. Predicted RSSI)

Abbreviations

3GPP	3rd Generational Partnership Project

References

1. Liu, Y.; Yang, H.; and Huang, R. (2022). Mobile user trajectory prediction based on machine learning. *Proceedings of* 2022 *IEEE* 95*th Vehicular Technology Conference* (*VTC*2022-*Spring*), Helsinki, Finland, 1-5.
2. Jiang, Z. (2024). Several applications of convolutional neural networks in medical imaging. *Transactions on Computer Science and Intelligent Systems Research*, 7.
3. Reis, R.K.D.; Damasceno, M.G.; and Arnez, J.J. (2024). Trajectory-based handover cell selection algorithm using GRU model in 5G networks. *Proceedings of* 2024 20*th International Conference on Wireless and Mobile Computing, Networking and Communications* (*WiMob*), Paris, France, 603-606.
4. Mahjoub, S.; Chrifi-Alaoui, L.; Marhic, B.; and Delahoche, L. (2022). Predicting energy consumption using LSTM, multi-layer GRU and drop-GRU neural networks. *Sensors*, 22(11), 4062.
5. Azoulay, R.; Edery, E.; Haddad, Y.; and Rozenblit, O. (2023). Machine learning techniques for received signal strength indicator prediction. *Intelligent Data Analysis*: *An International Journal*, 27, 1167-1184.
6. Kaur, G.; Goyal, R.K.; and Mehta, R. (2022). An efficient handover mechanism for 5G networks using hybridization of LSTM and SVM. *Multimedia Tools and Applications*, 81, 37057-37085.
7. Lu, S. et al. (2021). Exploring support vector machines for big data analyses. *Proceedings of the 4th International Conference on Computer Science and Software Engineering*, 31-37.
8. Song, Y.; Liang, J.; Lu, J.; and Zhao, X. (2017). An efficient instance selection algorithm for k nearest neighbor regression. *Neurocomputing*, 251, 26-34.
9. Lin, W. et al. (2022). A novel method to determine the handover threshold based on reconfigurable factor graph for LEO satellite internet network. *IEEE Access*, 10, 31907-31921.
10. Gaur, G.; Velmurugan, T.; Periasamy, P.; and Nandakumar, S. (2020). Application specific thresholding scheme for handover reduction in 5G Ultra Dense networks. *Telecommunication Systems*, 76, 97 - 113.
11. Liu, F.-H.F.; and Shih, S.-C. (2024). Algorithms for multi-criteria decision-making and efficiency analysis problems. *Arxiv preprint arXiv*:2406.06090.
12. Boström, H. (2024). Example-based explanations of random forest predictions. *Proceedings of* 22*nd International Symposium on Intelligent Data Analysis*, Stockholm, Sweden, 185-186.
13. Rifki, M.I.; Ikhwan, A.; and Muhammad, F. (2024). Performance evaluation of RSSI prediction methods in wireless communication networks. *ZERO: Jurnal Sains, Matematika dan Terapan*, 8(1), 14-25.
14. Dong, Z.Y.; Xu, W.M.; and Zhuang, H. (2019). Research on ZigBee Indoor Technology Positioning Based on RSSI. *Procedia Computer Science*, 154, 424–429.
15. Hastie, T.; Tibshirani, R.; and Friedman, J. (2008). Random forests. *The Elements of Statistical Learning*, 587-604.

16. Premkumar, G.R.V.; and Scoy, B.V. (2025). Optimal positioning of unmanned aerial vehicle (UAV) base stations using mixed-integer linear programming. *Drones*, 9(1), 44.
17. Yang, J.; Chen, Y.; Du, S.; Chen, B.; and Principe, J.C. (2024). IA-LSTM: interaction-aware LSTM for pedestrian trajectory prediction. *IEEE Transactions on Cybernetics*, 54(7), 3904-3917.
18. Aarif, L.; Tabaa, M.; and Hachimi, H. (2024). RSSI prediction for improved LoRa communications performance. *Proceedings of* 2024 *IEEE* 12*th International Symposium on Signal, Image, Video and Communications* (*ISIVC*), Marrakech, Morocco, 1-7.
19. Goldoni, E.; Savazzi, P.; Favalli, L.; and Vizziello, A. (2022). Correlation between weather and signal strength in LoRaWAN networks: An extensive dataset. *Computer Networks*, 202, 108627.
20. Mohsan, S.A.H.; Othman, N.Q.H.; Li, Y.; Alsharif, M.H.; and Khan, M.A. (2023). Unmanned aerial vehicles (UAVs): practical aspects, applications, open challenges, security issues, and future trends. *Intelligent Service Robotics*, 16, 109 - 137.
21. Savkin, A.V.; Huang, C.; and Ni, W. (2023). On-demand deployment of aerial base stations for coverage enhancement in reconfigurable intelligent surface-assisted cellular networks on uneven terrains. *IEEE Communications Letters*, 27(2), 666-670.
22. Viet, P.Q.; and Romero, D. (2022). Aerial base station placement: A tutorial introduction. *IEEE Communications Magazine*, 60(5), 44-49.
23. Firyaguna, F.; Lin, C.-K.; Alshaer, H.; and Harris, P. (2024). Graph-based handover for future aeronautical 6G integrated terrestrial and non-terrestrial networks. *Proceedings of* 2024 *AIAA DATC/IEEE* 43*rd Digital Avionics Systems Conference* (*DASC*), San Diego, CA, USA, 1-8.
24. Kosmopoulos, I.; Skondras, E.; Michalas, A.; Michailidis, E.T.; and Vergados, D.D. (2022). Handover management in 5G vehicular networks. *Future Internet*, 14(3), 87.
25. Guo, Y.; and Zhang, H. (2023). 3D boundary modeling and handover analysis of aerial users in heterogeneous networks. *IEEE Transactions on Vehicular Technology*, 72(10), 13523-13529.
26. Shayea, I. et al. (2022). Handover management for drones in future mobile networks - A survey. *Sensors*, 22(17), 6424.
27. Ma, Y.; Chen, X.; and Zhang, L. (2021). Base station handover based on user trajectory prediction in 5G networks. *Proceedings of* 2021 *IEEE International Conference on Parallel & Distributed Processing with Applications, Big Data & Cloud Computing, Sustainable Computing & Communications, Social Computing & Networking* (*ISPA/BDCloud/SocialCom/SustainCom*), New York City, NY, USA, 1476-1482.